Fermi surfaces without quasiparticles

Subir Sachdev

Department of Physics, Harvard University, Cambridge MA 02138, USA

(Dated: June 24, 2024)

Abstract

The general theory of a two-dimensional Fermi surface of quasiparticles coupled to a gapless scalar is presented. A systematic large N expansion is possible when the fermion-scalar Yukawa coupling is random in flavor space. Such a theory is shown to exhibit a Fermi surface which is sharp in momentum space, but broad in frequency because of the absence of coherent quasiparticle excitations. A model with the an additional spatial randomness in the Yukawa coupling has a linear in temperarture resistivity at the lowest temperatures.

`Chapter 34 from` *Quantum Phases of Matter*`, by S. S.`

`Cambridge University Press`

The SYK model of Chapter **??** has provided significant insights into the structure of metallic phases without quasiparticle excitations. However, such a theory has no spatial structure, and so no Fermi surface-like feature similar to that observed in the strange metal phase of the cuprates. This chapter will draw upon the insights gained in Chapter **??**, and describe more realistic models of metals without quasiparticle excitations with spatial structure. In the presence of full translational symmetry such models do have sharp Fermi surfaces in momentum space at $T = 0$. The absence of quasiparticles only makes them diffuse in energy space, but the location of the Fermi surface is well defined in momentum space, it is still given by (**??**). We will also consider the influence of spatial disorder on the sharp Fermi surface: this makes the Fermi surface diffuse also in momentum space, and is essential for a theory of the transport properties.

One of our main results will be the form of the Green's function in (23) for the Fermi surface without quasiparticles in two spatial dimensions in the absence of spatial disorder. We note that this Green's function is very different from that in (**??**) for the one-dimensional Tomonaga Luttinger liquid. This is evidence that it is not valid to think of the higher dimensional Fermi surface as a collection of independent one-dimensional quantum systems along each direction orthogonal to the Fermi surface. Rather, the correct description is in terms of overlapping patches at points on the Fermi surface, as we will show in Section I B. The structure of the Green's function in (23) is much closer to that of the SYK model, with a purely frequency-dependent *local* self energy in the large N limit of Section I A : we only have to add a smooth momentum-dependent bare energy to a purely local SYK-like self energy.

We will present our discussion in the context of a simple model for the onset of Ising ferromagnetism in a two-dimensional metal which is introduced Section I. However, the results are far more general, and apply to a wide class of models in which the Fermi surface is coupled to a gapless bosonic mode in two spatial dimensions. This includes

(i) the onset of Ising-nematic order in a Fermi liquid,

(ii) the U(1) spin liquid with a spinon Fermi surface that we briefly noted below (**??**), in which the Fermi surface excitations are coupled to a U(1) gauge field, and

(iii) the Halperin-Lee-Read state of a half-filled Landau level, which was noted in Sections **??** and **??**.

We will discuss the extension to these cases in Section III.

Our main tool for analyzing these problems will be a recently introduced large N approach which is directly inspired by the SYK model. This method will be described in Section I A, and leads to the analog of a G-Σ theory with a large N saddle point. Section I B will then describe how an exact low energy solution of the saddle-point equations can be obtained for the case without spatial disorder: this solution describes a sharp Fermi surface without quasiparticle excitations.

The other sections describe further properties of the sharp Fermi surface. Section II shows that the volume enclosed by the Fermi surface obeys the usual Luttinger relation, despite the absence of quasiparticles. Section IV considers pairing instabilities of the sharp Fermi surface, using methods closely related to those presented in Section **??** for the SYK model.

I. ONSET OF ISING FERROMAGNETISM

As our simplest example of a Fermi surface without quasiparticles, we consider the onset of ferromagnetic order in a two-dimensional metal. We assume that spin-orbit couplings render the spin correlations anisotropic in spin space, so that we can focus on only the z (say) component of the ferromagnetic order. We will use the framework of the paramagnon theory employed in Section **??** to describe the onset of spin density wave order at a wavevector $\boldsymbol{K} = (\pi, \pi)$, as in (**??**). In its original formulation [1, 2], the paramagnon theory was introduced as a theory of ferromagnetic spin fluctuations in liquid ^{3}He, and in such a theory we should take $\boldsymbol{K} = (0, 0)$. This requires that the underlying band structure and density of the electrons is such that the Lindhard susceptibility in (**??**) has a maximum at zero wavevector. We account for the anisotropy in spin space by including only the field $\phi \equiv \Phi_z$ in our low energy theory. Recent quantum Monte Carlo studies [3, 4] have examined an Ising model in a transverse field coupled to Fermi surfaces of electrons, and observed the onset of Ising magnetic order at a continuous quantum phase transition: the theory presented here is expected to describe such a transition.

The field theory for such a transition is obtained by the same route as that followed in Section **??**. We combine the free fermion theory in (**??**) with the scalar field theory for ϕ in (**??**) to obtain the Lagrangian

$$
\begin{aligned}
\mathcal{L} = \sum_{\boldsymbol{k},\alpha} c_{\boldsymbol{k},\alpha}^\dagger \left[\frac{\partial}{\partial \tau} + \varepsilon(\boldsymbol{k}) \right] c_{\boldsymbol{k},\alpha} + \int d^2 r \left\{ \frac{1}{2} \left[(\boldsymbol{\nabla} \phi)^2 + (\partial_\tau \phi)^2 + s\, \phi^2 \right] + \frac{u}{4!} \phi^4 \right\} \\
- \int d^2 r \, g \, \phi \, c_\alpha^\dagger \sigma^z_{\alpha\beta} c_\beta
\end{aligned}
\tag{1}
$$

We have allowed for an arbitrary dispersion of the electrons $c_{\boldsymbol{k}\alpha}$ in momentum space, with a Fermi surface at $\varepsilon_{\boldsymbol{k}} = 0$. However, we only include long-wavelength fluctuations in ϕ and so have performed a gradient expansion in its Lagrangian. The electrons are coupled to ϕ via the Yukawa coupling g, with σ^z the Pauli matrix. A crucial property of this Yukawa coupling is that it acts at zero momentum, unlike the non-zero momentum shift in (**??**). Other cases with a zero momentum order parameter lead to essentially the same results as we will describe below.

There has been a great deal of work [5] on theory (1), based essentially on a renormalized expansion in powers of g, supplemented by a large number of fermion flavors. This work has lead to numerous insights on the properties of (1), but has not led to a formulation in terms of a saddle-point theory which can be used to systematically classify the nature of higher order corrections.

A. Large N theory

Following the example of the SYK model, it was argued [6–8] that problems of fermions coupled to a critical boson could also be addressed by examining ensembles of theories with different Yukawa couplings. It is also possible to choose the ensemble so that the couplings are spatially independent, and this maintains full translational symmetry in each member of the ensemble. If most members of the ensemble flow to the same universal low energy theory, then we can access the low energy behavior by studying the average over the ensemble. We also obtain the added benefit of a G-Σ action with large N prefactor, which allows for a systematic treatment of the theory.

We will consider the following generalization of the theory (1)

$$\mathcal{L} = \sum_{\alpha=1}^{N} \sum_{\boldsymbol{k}} c_{\boldsymbol{k},\alpha}^{\dagger} \left[\frac{\partial}{\partial \tau} + \varepsilon(\boldsymbol{k}) \right] c_{\boldsymbol{k},\alpha} + \int d^2 r \sum_{\gamma=1}^{M} \left\{ \frac{1}{2} \left[(\boldsymbol{\nabla} \phi_\gamma)^2 + (\partial_\tau \phi_\gamma)^2 + s\, \phi_\gamma^2 \right] \right\} - \int d^2 r \sum_{\gamma=1}^{M} \sum_{\alpha,\beta=1}^{N} \frac{g_{\alpha\beta\gamma}}{N} \phi_\gamma \, c_\alpha^\dagger c_\beta \,. \tag{2}$$

Here the fermion has N components, the boson has M components, and we take the large N limit with

$$\lambda = \frac{M}{N} \tag{3}$$

fixed. The Yukawa coupling is taken to be a random function of the flavor indices with

$$\overline{g_{\alpha\beta\gamma}} = 0 \,, \quad g_{\alpha\beta\gamma}^{*} = g_{\beta\alpha\gamma} \,, \quad \overline{|g_{\alpha\beta\gamma}|^2} = g^2 \,. \tag{4}$$

We have dropped the quartic self-coupling u of the the scalar field for simplicity: it is unimportant for the leading critical behavior, but is needed for certain sub-leading effects at non-zero temperature [8]. The original theory in (1) has a $\phi \to -\phi$ symmetry which is only statistically present in (2): we can maintain this symmetry in each member of the ensemble by dividing the indices into groups of 2, but we avoid this complexity because it does not modify the large N results. We consider an ensemble of complex couplings because it simplifies the analysis, but real couplings lead to essentially the same results.

We can now proceed with the large N analysis following the script of the SYK model. As in Section **??**, the large N saddle point equations are most easily obtained by a diagrammatic perturbation theory in g, in which we average each graph order-by-order. In the large N limit, only the graphs shown in Fig. 1 survive, and yield the following saddle point equations

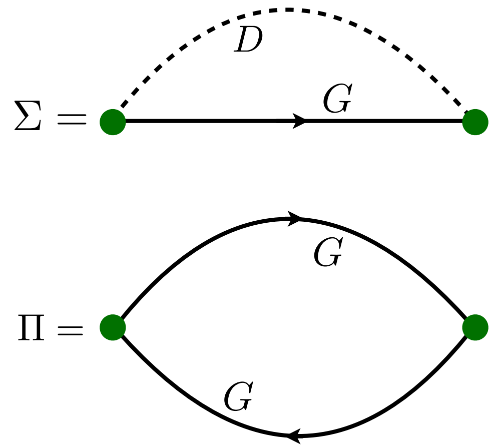

FIG. 1. Saddle point equations for the fermion self energy Σ and boson self energy Π, expressed in terms of the renormalized fermion Green's function G and boson Green's function D. The filled circle is the Yukawa coupling $g_{\alpha\beta\gamma}$.

$$
\begin{aligned}
\Sigma(\boldsymbol{r},\tau) &= g^2 \lambda D(\boldsymbol{r},\tau) G(\boldsymbol{r},\tau), \\
\Pi(\boldsymbol{r},\tau) &= -g^2 G(-\boldsymbol{r},-\tau) G(\boldsymbol{r},\tau), \\
G(\boldsymbol{k}, i\omega_n) &= \frac{1}{i\omega_n - \varepsilon(\boldsymbol{k}) - \Sigma(\boldsymbol{k}, i\omega_n)}, \\
D(\boldsymbol{q}, i\Omega_m) &= \frac{1}{\Omega_m^2 + q^2 + s - \Pi(\boldsymbol{q}, i\Omega_m)}.
\end{aligned} \tag{5}
$$

Here G is the Green's function for the fermion c, and Σ its self energy, and D is the Green's function for the boson f, and Π is its self energy.

The equations (5) are the analog of the SYK equations in (**??**-**??**), but the Green's functions now involve both spatial and temporal arguments. Remarkably, as we shall see in Section I B, an exact solution of the low energy scaling behavior is possible for (5), just as it was for the SYK model.

For completeness, we also write down the path integral of the averaged theory using bilocal Green's functions, the analog of (**??**) for the SYK model. We introduce the spacetime co-ordinate $X \equiv (\tau, x, y)$, and all Green's functions and self energies in the path integral are functions of two spacetime co-ordinates X_1 and X_2. Then we have

$$
\begin{aligned}
\overline{\mathcal{Z}} = \int & \mathcal{D}G(X_1,X_2)\mathcal{D}\Sigma(X_1,X_2)\mathcal{D}D(X_1,X_2) \\
& \times \mathcal{D}\Pi(X_1,X_2) \exp\left[-N I(G,\Sigma,D,\Pi)\right] .
\end{aligned} \tag{6}
$$

The G-Σ-D-Π action is now

$$\begin{aligned} I(G,\Sigma,D,\Pi) &= \frac{g^2\lambda}{2}\mathrm{Tr}\left(G\cdot[GD]\right) - \mathrm{Tr}(G\cdot\Sigma) + \frac{\lambda}{2}\mathrm{Tr}(D\cdot\Pi) \\ &- \ln\det\left[(\partial_{\tau_1} + \varepsilon(-i\boldsymbol{\nabla}_1))\,\delta(X_1 - X_2) + \Sigma(X_1,X_2)\right] \\ &\quad + \frac{\lambda}{2}\ln\det\left[\left(-\partial_{\tau_1}^2 - \boldsymbol{\nabla}_1^2 + s\right)\delta(X_1-X_2) - \Pi(X_1,X_2)\right]\,. \end{aligned} \tag{7}$$

where we have introduced notation analogous to (**??**)

$$\mathrm{Tr}\left(f\cdot g\right) \equiv \int dX_1 dX_2\, f(X_2,X_1) g(X_1,X_2)\,. \tag{8}$$

Note the crucial pre-factor of N before I in the path-integral. It can be verified that the saddle point equations of (7) reduce to (5).

B. Patch solution

This subsection will present an exact solution of the saddle point equations (5) in the low energy scaling limit. We will be able to obtain this solution for an arbitrary $\varepsilon(\boldsymbol{k})$, and for a general shape of the Fermi surface. The key to the solution is the observation that the singular behavior at any point on the Fermi surface is determined only by a small momentum space patch around it, as well as that of the anti-podal point. We do need to include the curvature of the Fermi surface though, and it is not sufficient to think of the Fermi surface as a set of one-dimensional chiral fermions at each point on the Fermi surface.

We begin by evaluating Π in (5) using the bare fermion Green's function. This yields the Lindhard susceptibility in (**??**) and (**??**)

$$\begin{aligned} \Pi(\boldsymbol{q}, i\Omega_m) &= -g^2 T\sum_{\omega_n}\int\frac{d^2k}{4\pi^2}\frac{1}{(i(\omega_n+\Omega_m) - \varepsilon(\boldsymbol{k}+\boldsymbol{q}))(i\omega_n - \varepsilon(\boldsymbol{k}))} \\ &= g^2\int\frac{d^2k}{4\pi^2}\frac{f(\varepsilon(\boldsymbol{k}+\boldsymbol{q})) - f(\varepsilon(\boldsymbol{k}))}{i\Omega_m + \varepsilon(\boldsymbol{k}) - \varepsilon(\boldsymbol{k}+\boldsymbol{q})}\,, \end{aligned} \tag{9}$$

where $f(\varepsilon)$ is the Fermi function. We are interested in the behavior of Π for small $\boldsymbol{q}$ and Ω_m at low T. On the real frequency axis, the real part of Π is not universal , and depends in a complicated manner on the entire fermion dispersion. However, the behavior of the imaginary part of Π is much simpler and universal. We have

$$\begin{aligned} \mathrm{Im}\,\Pi(\boldsymbol{q},\Omega) &= -\pi g^2\int\frac{d^2k}{4\pi^2}\left[f(\varepsilon(\boldsymbol{k}+\boldsymbol{q})) - f(\varepsilon(\boldsymbol{k}))\right]\delta\left(\Omega + \varepsilon(\boldsymbol{k}) - \varepsilon(\boldsymbol{k}+\boldsymbol{q})\right) \\ &= \pi g^2\Omega\int\frac{d^2k}{4\pi^2}\,\delta\left(\varepsilon(\boldsymbol{k})\right)\delta\left(\Omega + \varepsilon(\boldsymbol{k}) - \varepsilon(\boldsymbol{k}+\boldsymbol{q})\right) \quad \text{as } T\to 0. \end{aligned} \tag{10}$$

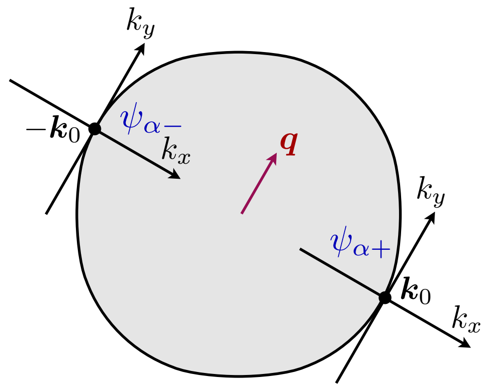

FIG. 2. Points $\pm\boldsymbol{k}_0$ on the Fermi surface which satisfy (11). The momentum of the boson is $\boldsymbol{q}$, and the low energy fermion contributions arise from momenta in the vicinity of $\pm\boldsymbol{k}$.

The last expression contains an integral over 2-dimensional momentum space of $\boldsymbol{k}$, along with 2 delta functions containing arguments which are functions of $\boldsymbol{k}$. Generically, both delta functions will be satisfied only at isolated points in momentum space. For $|\boldsymbol{q}|, |\Omega| \to 0$, the isolated points are solutions of

$$\varepsilon(\boldsymbol{k}) = 0 \quad \text{and} \quad \boldsymbol{q} \cdot \boldsymbol{\nabla}_{\boldsymbol{k}} \varepsilon(\boldsymbol{k}) = 0 \,. \tag{11}$$

The solution of (11) is illustrated in Fig. 2: for a simply connected, convex Fermi surface, each direction of $\boldsymbol{q}$ is identified with the 2 anti-podal points $\pm\boldsymbol{k}_0$ on the Fermi surface where $\boldsymbol{q}$ is parallel to the tangent to the Fermi surface. Note that the value of $\boldsymbol{k}_0$ is fully determined by $\boldsymbol{q}$, but we leave this dependence implicit.

As illustrated in Fig. 2, we choose our momentum space axes so that $\boldsymbol{q} = (0, q_y)$. In the vicinity of $\boldsymbol{k}_0$ we write the fermion dispersion near the Fermi surface patch at $\boldsymbol{k}_0$ as

$$\boldsymbol{k} = \boldsymbol{k}_0 + (k_x, k_y), \quad \varepsilon(\boldsymbol{k}) = v_F k_x + \frac{\kappa}{2} k_y^2 \,, \tag{12}$$

whereas near $-\boldsymbol{k}_0$ we have

$$\boldsymbol{k} = -\boldsymbol{k}_0 + (k_x, k_y), \quad \varepsilon(\boldsymbol{k}) = -v_F k_x + \frac{\kappa}{2} k_y^2 \,. \tag{13}$$

Here v_F is the Fermi velocity, and κ is the curvature of the Fermi surface. The values of v_F and κ depend upon $\boldsymbol{k}_0$ which in turn depends upon $\boldsymbol{q}$, and they will vary as $\boldsymbol{k}_0$ moves around the Fermi surface, but we have not explicitly indicated that; our results will remain valid even in the presence of such variation. We can now insert (12) into (10) and obtain the Landau damping result

$$\begin{aligned} \mathrm{Im}\, \Pi(\boldsymbol{q}, \Omega) &= 2\pi g^2 \Omega \int \frac{d^2k}{4\pi^2}\, \delta\left(v_F k_x + \kappa k_y^2/2\right) \delta\left(\kappa k_y q_y + q_y^2/2 - \Omega\right) \\ &= \frac{g^2 \Omega}{2\pi v_F \kappa |q_y|} \end{aligned} \tag{14}$$

where the leading factor of 2 is from the sum over the anti-podal points. Note that the curvature κ appears in the denominator, and so it is not valid to take the $\kappa \to 0$ limit, and no description in terms of purely linearly-dispersing excitations around the Fermi surface is possible.

Let us now turn to an evaluation of Π in (5) using the fully renormalized Green's function. Remarkably, as we will now show, the result in (14) remains largely unchanged. We anticipate that full solution of (5) leads to a fermion Green's function of the following form

$$\Sigma(\boldsymbol{k}, i\omega_n) = \Sigma_0(\boldsymbol{k}) + \Sigma(i\omega_n) \tag{15}$$

The momentum dependence of $\Sigma_0(\boldsymbol{k})$ will be non-singular, and we assume it can be absorbed by redefinition of the values of v_F and κ; we will therefore not include it in the computations below. The frequency dependent part $\Sigma(i\omega_n)$ can be singular (as we will see below) but it has no dependence on k_x and k_y; however it will depend upon the choice of $\boldsymbol{k}_0$, via the implicit $\boldsymbol{k}_0$ dependence of v_F and κ. We now insert $\Sigma(i\omega_n)$ into the first expression in (9) and use the dispersion (12) to obtain

$$\begin{aligned}\Pi(\boldsymbol{q}, i\Omega_m) = -2g^2 T \sum_{\omega_n} \int \frac{d^2k}{4\pi^2} & \frac{1}{(i\omega_n - v_F k_x - \kappa q_y^2/2 - \Sigma(i\omega_n))} \\ \times & \frac{1}{(i(\omega_n + \Omega_m) - v_F k_x - \kappa(k_y + q_y)^2/2 - \Sigma(i\omega_n + i\Omega_m))} \,. \end{aligned} \tag{16}$$

At this point in (9) we evaluated the summation over the frequency ω_n, but we are unable to do that here because of the unknown frequency dependence in $\Sigma(i\omega_n)$. So we have instead decided to focus only on the contribution of the patches near $\pm\boldsymbol{k}_0$, and linearized the fermion dispersion accordingly. In this situation the dependence of the integrand on k_x and k_y is simple. Performing the integral over k_x in (16) we obtain

$$\begin{aligned}\Pi(\boldsymbol{q}, i\Omega_m) = \frac{-ig^2 T}{v_F} \sum_{\omega_n} \int \frac{dk_y}{(2\pi)} & \left[\text{sgn}(\omega_n + \Omega_m) - \text{sgn}(\omega_n)\right] \\ & \times \frac{1}{i\Omega_m - \kappa q_y^2/2 - \kappa q_y k_y + \Sigma(i\omega_n) - \Sigma(i\omega_n + i\Omega_m)} \,. \end{aligned} \tag{17}$$

We have assumed here that $\text{sgn}(\omega_n - \Sigma(i\omega_n)/i) = \text{sgn}(\omega_n)$, and this always turn out to be the case from the positivity requirements of the fermion spectral weight. The next step is the evaluation of the q_y integral in (17). The real part of this integral is logarithmically divergent at large q_y, but then we are no longer in a regime where it is valid to keep the linearized dispersion. We assume that the divergent pieces only yield non-singular contribution, and keep the singular imaginary part of the integral. In this manner, we obtain from (17)

$$\begin{aligned}\Pi(\boldsymbol{q}, i\Omega_m) &= \frac{g^2 T}{2\kappa v_F |q_y|} \sum_{\omega_n} \text{sgn}(\Omega_m) \left[\text{sgn}(\omega_n + \Omega_m) - \text{sgn}(\omega_n)\right] \\ &= -\frac{g^2 |\Omega_m|}{2\pi \kappa v_F |q_y|} \,. \end{aligned} \tag{18}$$

This agrees precisely with (14), and all dependence on Σ has dropped out, as we claimed.

The final step in the exact solution of (5) is the evaluation of $\Sigma(i\omega_n)$ at the point $\boldsymbol{k}_0$ on the Fermi surface. As we noted earlier, the parameters v_F and κ depend smoothly upon the choice of $\boldsymbol{k}_0$, and this will be the only momentum dependence in the singular part of the fermion self energy. A careful evaluation first proceeds by the real frequency method used for Π in (10), and we can follow that method for the imaginary part of the $\Sigma(\omega)$ on the real frequency axis. Such an evaluation shows that the result is dominated by the fermions in the vicinity of $\boldsymbol{k}_0$, and with boson momentum $q_y \gg q_x$ which is nearly tangent to the Fermi surface. However, we proceed directly to the second method used for Π below (16) in which we integrate over momenta before we integrate over frequency: this has the advantage of allowing use to include $\Sigma(i\omega_n)$ in the fermion propagator. From the first equation in (5), using the linearized dispersion and result above, we have

$$\Sigma(\boldsymbol{k}, i\omega_n) = g^2 \lambda \int \frac{d^2 q}{(2\pi)^2} T \sum_{\Omega_m} \frac{1}{q_y^2 + s + \dfrac{g^2 |\Omega_m|}{2\pi v_F \kappa |q_y|}}$$
$$\times \frac{1}{i(\Omega_m + i\omega_n) - v_F(k_x + q_x) - \kappa(k_y + q_y)^2/2 - \Sigma(i\Omega_m + i\omega_n)} . \qquad (19)$$

where we have dropped q_x in the boson propagator. We can now perform the integral over q_x, and observe that the expression is indeed independent of $\boldsymbol{k}$, and the frequency dependent Σ in the denominator. So we have our closed-form expression for the fermion self energy

$$\Sigma(i\omega_n) = -i \frac{g^2 \lambda}{2 v_F} \int \frac{dq_y}{2\pi} T \sum_{\Omega_m} \frac{\operatorname{sgn}(\omega_n + \Omega_m)}{q_y^2 + s + \dfrac{g^2 |\Omega_m|}{2\pi v_F \kappa |q_y|}} . \qquad (20)$$

We are interested in the singular behavior of this fermion self energy at the critical point $s = 0$. At $T > 0$, we have to account for thermal effects arising from the boson self-interaction u in (1) which make the renormalized s temperature dependent. We will not discuss these subtle issues [7–10] here, and limit ourselves below to $T = 0$.

For $s > 0$ and $T = 0$, evaluation of the integrals over q_y and Ω in (20) shows that $\text{Im}\Sigma(\omega) \sim -(\omega/s)^2 \ln(1/|\omega|)$, which is the expected behavior for a two-dimensional Fermi liquid (see QPT book). At the critical point $s = 0$, and at $T = 0$, we perform the q_y integral, and then the frequency integral to obtain

$$\begin{aligned}\Sigma(i\omega) &= -i \frac{g^2 \lambda}{3 v_F \sqrt{3}} \left(\frac{2\pi v_F \kappa}{g^2} \right)^{1/3} \int \frac{d\Omega}{2\pi} \frac{\operatorname{sgn}(\omega + \Omega)}{|\Omega|^{1/3}} \\ &= -iB \operatorname{sgn}(\omega) |\omega|^{2/3} \quad s = 0, T = 0 ,\end{aligned} \qquad (21)$$

with

$$B = \frac{g^2 \lambda}{2\pi v_F \sqrt{3}} \left(\frac{2\pi v_F \kappa}{g^2} \right)^{1/3} . \qquad (22)$$

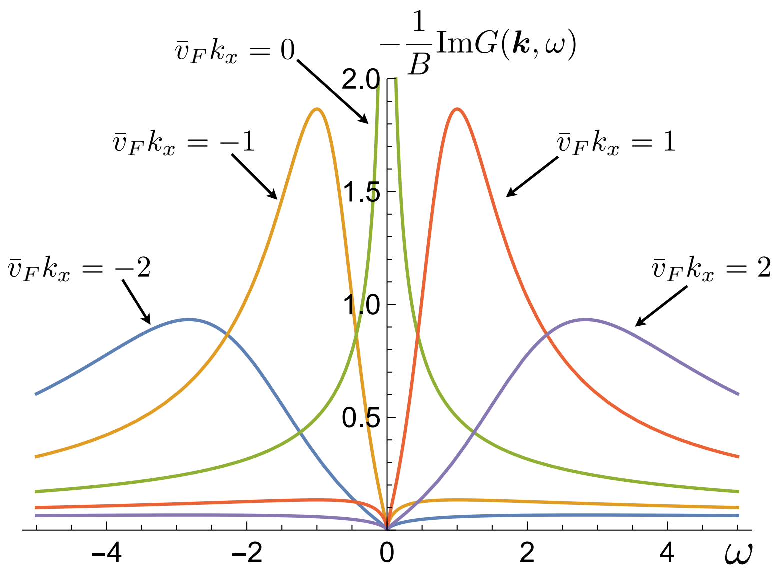

FIG. 3. Plot of fermion spectral density from (23) at wavevectors $\boldsymbol{k} = \boldsymbol{k}_0 + (k_x, 0)$ across the Fermi surface without quasiparticles. Here $\bar{v}_F = v_F/B$.

It is instructive to examine the frequency and momentum dependence of the $T = 0$ fermion Green's function across the Fermi surface. In the scaling limit, we can write the real frequency axis Green's function near the Fermi surface as

$$G(\boldsymbol{k}, \omega) = \frac{1}{-v_F k_x - \kappa k_y^2/2 + iBe^{-i\pi \mathrm{sgn}(\omega)/3}|\omega|^{2/3}} \,. \tag{23}$$

As in the SYK model, we can drop the bare ω term in G^{-1} because it is subleading with respect to the frequency-dependent self energy. Note also the distinction in the singularity structure from (**??**) for the one-dimensional Tomonaga Luttinger liquid—the singularity here is entirely in the frequency dependence of the self energy, as in the SYK model. We show a plot of $-\mathrm{Im}G$ in Fig. 3. On the Fermi surface $k_x = 0$, $k_y = 0$ we have $\mathrm{Im}G \sim -1/|\omega|^{2/3}$, which is similar to the $\mathrm{Im}G \sim -1/|\omega|^{1/2}$ behavior of the SYK model. Unlike the Fermi liquid, there is no delta function in ω on the Fermi surface, indicating the absence of quasiparticles. Away from the Fermi surface, $\mathrm{Im}G$ actually vanishes on the Fermi surface (see Fig. 3), and there is a broad spectral feature which disperses as $\omega = [(2v_F/(\sqrt{3}B))k_x]^{2/3}$. Note that the position of the Fermi surface is still given by the vanishing of the inverse Green's function at zero frequency, as in (**??**).

We can compute the momentum distribution function of the electrons from (23), and it leads to result similar in form to that of a Tomonaga-Luttinger liquid in (**??**)

$$n(\boldsymbol{k}) \sim -\mathrm{sgn}(v_F k_x + \kappa k_y^2/2)|v_F k_x + \kappa k_y^2/2|^{1/2} \,, \tag{24}$$

with a power-law singularity on the Fermi surface. But recall that the frequency dependent form of (23) is quite different from (**??**) for the one-dimensional electron gas.

At non-zero T, the SYK model displays simple ω/T scaling in its spectral function. There are 'quantum' contributions which do indeed scale as ω/T for the critical Fermi surface, but there are also additional corrections which arise from classical thermal fluctuations of ϕ which are important. So the $T > 0$ situation is rather complex [7–10], as we noted above.

C. Patch field theory

Having obtained the analytic solution of the large N saddle point equations in (5) by the asymptotic low energy analysis above, it is natural to ask if the asymptotic analysis can be performed directly on the theory (2) so that we can understand the solution in terms of a more conventional scaling analysis on a quantum field theory. The analysis of the saddle point equations makes it clear that all the singular effects arise from the vicinity of the points $\pm\boldsymbol{k}_0$ on the Fermi surface for the case of a boson fluctuation in the direction $\boldsymbol{q}$, as shown in Fig. 2. So we introduce fermion fields $\psi_{\alpha\pm}$ in the vicinity of these points, and expand their dispersion in gradients according to (12) and (13). This yields the action [8, 11, 12]

$$\mathcal{S} = \int dx dy d\tau \, \mathcal{L}$$

$$\mathcal{L} = \sum_{\alpha=1}^{N} \left\{ \psi_{\alpha+}^\dagger \left[\partial_\tau - i\partial_x - (\kappa/2)\partial_y^2\right] \psi_{\alpha+} + \psi_{\alpha-}^\dagger \left[\partial_\tau + i\partial_x - (\kappa/2)\partial_y^2\right] \psi_{\alpha-} \right\}$$
$$+ \frac{1}{2}\sum_{\gamma=1}^{M} (\partial_y \phi_\gamma)^2 + \sum_{\gamma=1}^{M} \sum_{\alpha,\beta=1}^{N} \frac{g_{\alpha\beta\gamma}}{N} \phi_\gamma \left[\psi_{\alpha+}^\dagger \psi_{\beta+} + \psi_{\alpha-}^\dagger \psi_{\beta-}\right] . \quad (25)$$

We have dropped the x and τ gradient terms of ϕ in (2), anticipating they are irrelevant in the scaling analysis we now present.

We analyze the behavior of (25) under the rescaling transformation

$$x \to x/b\,, \quad y \to y/b^{1/2}\,, \quad \tau \to \tau/b^z\,, \quad (26)$$

where the rescaling of x and y leaves the fermion dispersion invariant, but we leave the dynamic critical exponent undetermined for now. Then the $(\partial_y\phi_\gamma)^2$ term is invariant if we choose

$$\phi \to \phi\, b^{(1+2z)/4}\,. \quad (27)$$

Similarly the spatial gradient terms of ψ are invariant if we choose

$$\psi \to \psi\, b^{(1+2z)/4}\,. \quad (28)$$

At this point, it is conventional to fix z by demanding the invariance of temporal gradient terms. However, we saw in our analysis that the bare ω term in G^{-1} was irrelevant, and we dropped it in (23), and so this is not the appropriate way to proceed. Instead we examine the scaling of the Yukawa coupling in (25), which is

$$g \to g\, b^{(3-2z)/4}\,. \tag{29}$$

At a critical fixed point, we expect g to be invariant, and this yields the value

$$z = \frac{3}{2}\,. \tag{30}$$

This is precisely the value we would have obtained by comparing the k_x and ω terms in (23).

The lesson is that we have to study the theory (25) at *fixed* g, and it is not permissible to expand in powers of g. We can regard this fixed g requirement as the analog of a non-linear sigma model constraint in more conventional quantum field theories.

The quantum field theory (25) can be used to compute corrections beyond the large N saddle point theory presented in Section I B. This has not yet been computed within the large N method of Section I A, but in an uncontrolled method which examines certain 3-loop graphs [12]: this leads to a small fermion anomalous dimension, and hence a breakdown of the purely local form of the singular electron self-energy. It is interesting to note that finite N corrections discussed in Section **??** also lead to a breakdown of the local scaling of the SYK model, although from a different mechanism involving the time reparameterization mode (there is no time reparameterization soft model for the Fermi surface being discussed here [8]).

Related scaling analyses can also be used in higher dimensions, and in particular for $d = 3$. A key feature in $d = 2$ is that both the fermion Green's function in (23), and the Landau-damped boson Green's function implied by (18), are characterized by the same dynamic critical exponent $z = 3/2$. A perturbative computation of the corresponding Green's functions in general d shows that the boson Green's function still has $z_b = 3/2$, while the fermion Green's function has $z_f = 3/d$ (see QPT book). For $d > 2$ we have $z_f < z_b$, and so at any given small wavevector, fermionic excitations are higher in energy than bosonic excitations: this implies that the fermions can be safely integrated out, and a perturbative analysis of the effective bosonic theory is valid.

II. LUTTINGER RELATION

The strong damping and breakdown of quasiparticles implied by (21) and (22) nevertheless does not remove the sharp Fermi surface. There is no singular momentum dependence in these expressions, and the frequency dependence still obeys (**??**). Consequently, there is still a Fermi surface specified by (**??**).

We now show that this Fermi surface obeys the same Luttinger relation as that of a Fermi liquid. The argument proceeds just as in Section **??**. The evaluation of (**??**) proceeds as before, as the self energy all the needed properties. We only need to examine more carefully the fate of the

Luttinger-Ward term in (??): in the SYK model, the corresponding term I_2 in (??) did not vanish. Here, the Green's function is momentum dependent, and the expression for I_2 has an additional momentum integral

$$I_2 = -i \int_{-\infty}^{\infty} \int \frac{d^2k}{4\pi^2} \frac{d\omega}{2\pi} G(\boldsymbol{k}, i\omega) \frac{d}{d\omega} \Sigma(i\omega) e^{-i\omega 0^+} \tag{31}$$

As the self energies of the SYK model and the critical Fermi surface both obey (??) with $\alpha < 1$, it is possible that there is an anomalous contribution at $\omega = 0$ that leads to a non-vanishing I_2. However, that is not the case here because the singularity of the Green's function is much weaker as a result of its momentum dependence; now the low energy Green's function is

$$G^{-1}(\boldsymbol{k}, i\omega) = -v_F k_x - \frac{\kappa}{2} k_y^2 - \Sigma(i\omega) \,, \tag{32}$$

and this diverges at $\omega = 0$ only on the Fermi surface $v_F k_x + \kappa k_y^2/2 = 0$. Indeed, with this form, the local density of states is a constant at the Fermi level. Consequently, there is no anomaly at $T = 0$, and $I_2 = 0$ from the Luttinger-Ward functional analysis. Incidentally, we note that the Luttinger-Ward functional in the large N limit is just the first term in the action I in Eq. (7), similar to the SYK model.

To complete this discussion, we add a few remarks on the structure of the Luttinger-Ward functional, and its connection to global U(1) symmetries [13, 14]. Consider the general case where there are multiple Green's functions (of bosons or fermions) $G_\alpha(k_\alpha, \omega_\alpha)$. Let the α'th particle have a charge q_α under a global U(1) symmetry. Then for each such U(1) symmetry, the Luttinger-Ward functional will obey the identity

$$\Phi_{LW} \left[G_\alpha(\boldsymbol{k}_\alpha, \omega_\alpha) \right] = \Phi_{LW} \left[G_\alpha(\boldsymbol{k}_\alpha, \omega_\alpha + q_\alpha \Omega) \right] . \tag{33}$$

Here, we are regarding Φ_{LW} as functional of two distinct sets of functions $f_{1,2\alpha}(\omega_\alpha)$, with $f_{1\alpha}(\omega_\alpha) \equiv G_\alpha(k_\alpha, \omega_\alpha + q_\alpha \Omega)$ and $f_{2\alpha}(\omega) \equiv G_\alpha(k_\alpha, \omega_\alpha)$, and Φ_{LW} evaluates to the same value for these two sets of functions. Expanding (33) to first order in Ω, and integrating by parts, we establish the corresponding $I_2 = 0$.

III. FERMI SURFACE COUPLED TO A GAUGE FIELD

As we noted in the beginning of this chapter, the problem of a Fermi surface coupled to a gauge field in 2+1 dimensions leads properties very similar to those of the Ising ferromagnet described by (1). This becomes clear when we reduce the field theory to a 2-patch theory along the lines of Section I B, as we will now describe. These results will be applicable to the U(1) spin liquid with a spinon Fermi surface noted below (??), and problem of the half-filled Landau level, noted in Sections ?? and ??.

Following the procedure in Section **??**, we can describe the problem of U(1) gauge field coupled to a Fermi surface by the following general Lagrangian (replacing (1))

$$\mathcal{L} = \sum_{\boldsymbol{k},\alpha} c^\dagger_{\boldsymbol{k},\alpha} \left[\frac{\partial}{\partial \tau} + \varepsilon(\boldsymbol{k} - g\boldsymbol{a}) \right] c_{\boldsymbol{k},\alpha} + \int d^2 r \left\{ \frac{K_\tau}{2} \left(\partial_\tau \boldsymbol{a}\right)^2 + \frac{K}{2} \left(\boldsymbol{\nabla} \times \boldsymbol{a}\right)^2 \right\} . \tag{34}$$

We focus only on the spatial components of the gauge field, as the temporal components are screened by the background charge density. We will also work in the Landau gauge

$$\boldsymbol{\nabla} \cdot \boldsymbol{a} = 0 \,. \tag{35}$$

We can now perform an analysis of the gauge field polarization from the fermion loop diagram using an analysis closely related to that in Section I B. As in Fig. 2, we find that a gauge field fluctuations at wavevector $\boldsymbol{q}$ is damped only by fermion excitations at the anti-podal points $\pm \boldsymbol{k}_0$. Using the condition (35) at this point, we can write the gauge field in terms of its single transverse component

$$\boldsymbol{a} = (\phi, 0) \,. \tag{36}$$

Now we take the long-wavelength limit, following the mapping from (2) to (25). The theory (34) yields the Lagrangian density

$$\begin{aligned} \mathcal{L} = \sum_\alpha & \left\{ \psi^\dagger_{\alpha +} \left[\partial_\tau - i \partial_x - (\kappa/2) \partial_y^2 \right] \psi_{\alpha +} + \psi^\dagger_{\alpha -} \left[\partial_\tau + i \partial_x - (\kappa/2) \partial_y^2 \right] \psi_{\alpha -} \right\} \\ & + \frac{K}{2} \left(\partial_y \phi\right)^2 + g \sum_\alpha \phi \left[\psi^\dagger_{\alpha +} \psi_{\alpha +} - \psi^\dagger_{\alpha -} \psi_{\alpha -} \right] \,. \end{aligned} \tag{37}$$

The key difference between (37) and (25) is in the relative sign of the two terms in the Yukawa coupling. This sign makes no difference to the analyses in Section I A, and so all previous results apply also to (34). However, we will see that this sign does make a crucial difference in the considerations of fermion pairing in Section IV.

IV. PAIRING CORRELATIONS

We now study possible pairing instabilities of the non-Fermi liquid states, analogous to the BCS pairing instability of Fermi liquids in Chapter **??**. As we are dealing with critical state without quasiparticle excitations, we will study the pairing correlations by a method analogous to that used to study composite operators of the SYK model in Section **??**. We will examine a large N equation analogous to Fig. **??**, and compute the scaling dimension of the Cooper pairing operator. If the value of the scaling dimension is real, then this gives us information on the correlation functions of the pairing operator in the non-Fermi liquid state. However, we will find that under suitable conditions the scaling dimension is complex. Following Refs. [15, 16], we will interpret the complex scaling dimension as in indication of an instability to a paired state.

To begin with, we can ignore the absence of quasiparticles, and consider pairing by exchange of ϕ between ψ_+ and ψ_-, along the lines of the paramagnon exchange in Section **??**. Such considerations show that the interaction is attractive (repulsive) between parallel (anti-parallel) spin particles for the Ising ferromagnetic case, and repulsive for arbitrary spin particles for the gauge fields case.

To go beyond such leading order results, and self-consistently include the absence of quasiparticles, it is important work with a systematic large N limit. So we generalize the patch theories in (25) and (37) to a theory with N flavors of fermions, M_1 flavors of bosons which mediate an attractive interaction (in the pairing channel) between antipodal points on the Fermi surface, and M_2 flavors of bosons which mediate a repulsive interaction. By rescaling the bosons, we will normalize the mean-square Yukawa coupling for both classes of bosons with the same value g; the value of g will drop out in the scaling equations we consider in this section. Having obtained the same Yukawa coupling, we do have to consider the co-efficient of the $(\partial_y \phi)^2$ term in (25) more carefully. We take this co-efficient to equal K_1 and K_2 for the two bosons, and we will see below that the ratio K_1/K_2 influences the critical exponents. For the gauge field case, the values of $K_{1,2}$ are equal to the corresponding diamagnetic susceptibility of the system [17], and this depends upon the lattice scale properties. So we have the theory

$$\mathcal{L} = \sum_{s=\pm 1} \sum_{\alpha=1}^{N} \psi_{\alpha s}^\dagger \left[\partial_\tau - is\partial_x - \partial_y^2 \right] \psi_{\alpha s} + \sum_{a=1,2} \frac{K_a}{2} \sum_{\gamma=1}^{M_a} \left(\partial_y \phi_{\gamma a} \right)^2 + \sum_{s=\pm 1} \sum_{a=1}^{2} s^{3-a} \sum_{\gamma=1}^{M_a} \sum_{\alpha,\beta=1}^{N} \frac{g_{\alpha\beta\gamma}^a}{N} \psi_{\alpha s}^\dagger \psi_{\beta s} \phi_{\gamma a} \,. \quad (38)$$

Here $s = \pm 1$ is the index of the two anti-podal patches (see Fig. 2), and $a = 1, 2$ represents the attractive and repulsive bosons respectively. Also, it will be necessary to take the random couplings $g_{\alpha\beta\gamma}^a$ to now be real independent variables.

Let us now recompute the boson and fermion self energies of Section I B for the theory (38). The self energy of the boson $\phi_{\gamma a}$ is still equal to (18), while the self energy of the fermion in (21) becomes

$$\Sigma(i\omega) = -i \frac{g^2}{2\pi\sqrt{3}} \left(\frac{M_1 K_1^{-2/3} + M_2 K_2^{-2/3}}{N} \right) \left(\frac{2\pi v_F \kappa}{g^2} \right)^{1/3} \text{sgn}(\omega) |\omega|^{2/3} \,. \quad (39)$$

We now consider the scaling dimension of the composite operator $\psi_{\alpha+}^\dagger \psi_{\alpha-}^\dagger$ along the lines of Section **??**. The large N limit leads to an integral equation for the pairing vertex, analogous to that in Fig. **??** and (**??**), shown in Fig. 4. We first consider the internal loop, and evaluate the integral over momenta along the lines of the analysis in Section I B, while assuming momentum

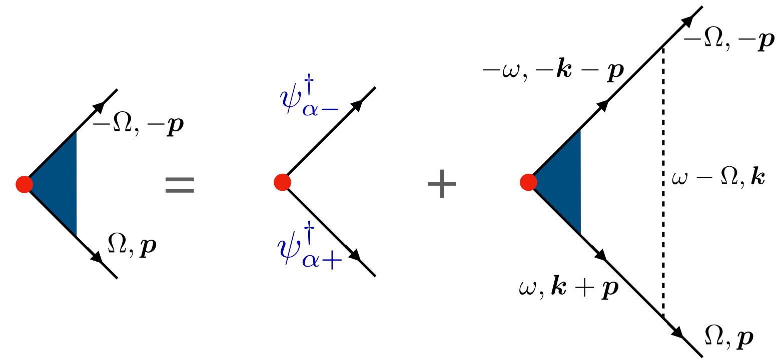

FIG. 4. Large N equation for the scaling dimension of the composite operator $\psi^\dagger_{\alpha+}\psi^\dagger_{\alpha-}$, leading to (42) after integration over the momentum in the loop of the last diagram. The filled triangle is the pairing vertex Δ.

independence of the vertex — we will see below that this assumption is consistent:

$$\int \frac{dk_x dk_y}{4\pi^2} \frac{1}{(i\omega - v_F(k_x+p_x) - \kappa(k_y+p_y)^2/2 - \Sigma(i\omega))} \\ \times \frac{1}{(-i\omega - v_F(k_x+p_x) - \kappa(k_y+p_y)^2/2 - \Sigma(-i\omega))(K_a k_y^2 + \Pi(k_y, i\omega - i\Omega))}\,. \tag{40}$$

Notice that the k_x term appears with the same sign in the two fermion propagators, while the frequencies have opposite signs, corresponding to the pairing between antipodal patches. This structure is crucial to the non-vanishing result of the k_x integral in (40), which yields

$$\int \frac{dk_y}{4\pi v_F} \frac{1}{|\omega + i\Sigma(i\omega)|(K_a k_y^2 + \Pi(k_y, i\omega - i\Omega))}\,. \tag{41}$$

This result is independent of the external momentum $\boldsymbol{p}$ — this implies we can consistently take the pairing vertex to be independent of momentum. The pairing vertex depends only upon frequency, just like the fermion self energy, and the situation is now essentially identical to that for the SYK model in Section **??**, with the composite operator also having only local correlations. We can perform the k_y integral in (41), and then Fig. 4 yields the following integral equation for the pairing vertex in frequency space alone

$$E\Delta(i\Omega) = -\sum_a \frac{M_a \zeta_a g^2}{3N\sqrt{3}} \int \frac{d\omega}{2\pi} \frac{\Delta(i\omega)}{|\omega + i\Sigma(i\omega)|} \frac{(4\pi)^{1/3}}{(gK_a)^{2/3}|\omega - \Omega|^{1/3}}\,. \tag{42}$$

Here $a = 1, 2$ sums over the attractive and repulsive bosons and $\zeta_a = 2a - 3 = -1$ $(+1)$ for the attractive (repulsive) interactions. Solutions of this equation with eigenvalue $E = 1$ will determine the scaling of $\Delta(i\Omega)$, as in (**??**). At low energies and $T = 0$, where we drop the bare ω term in the right hand side of (42), because it is irrelevant in the infrared (IR), we obtain a universal equation

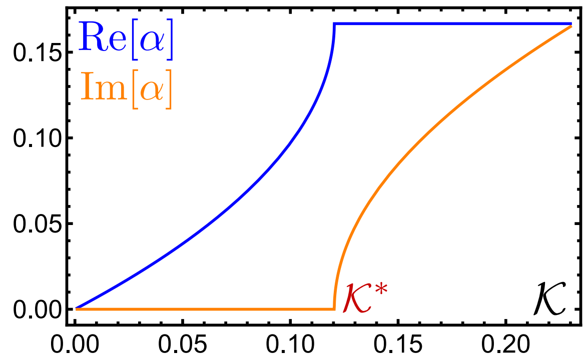

FIG. 5. Plot [8] of Re[α] and Im[α], for the solutions which have Re[α] $\leq 1/6$ and Im[α] > 0, as a function of $\mathcal{K}$. The critical Fermi surface is unstable to pairing for $\mathcal{K}^* < \mathcal{K} < 1$, where Re[$\alpha$] $= 1/6$ and Im[α] $\neq 0$. For $0 < \mathcal{K} < \mathcal{K}^*$, the pairing operator has a non-trivial scaling dimension determined by Re[α]. Reprinted with permission from APS.

independent of the coupling g

$$E\Delta(i\Omega) = \frac{\mathcal{K}}{3}\int \frac{d\omega}{2\pi}\frac{2\pi\Delta(i\omega)}{|\omega|^{2/3}|\omega-\Omega|^{1/3}}\,, \tag{43}$$

where the dimensionless constant

$$\mathcal{K} \equiv \frac{M_1 K_2^{2/3} - M_2 K_1^{2/3}}{M_1 K_2^{2/3} + M_2 K_1^{2/3}} \tag{44}$$

determines the balance between the attractive and repulsive interactions. The Ising ferromagnet case as $M_1 = 1$, $M_2 = 0$, $\mathcal{K} = 1$, while the gauge field case has $M_1 = 0$, $M_2 = 1$, $\mathcal{K} = -1$. Equation (43) has the same form as that for the $\gamma = 1/3$ case of the γ-model of quantum-critical pairing studied by Chubukov and collaborators [18–21].

As in Section **??**, we assume the eigenvector has the form

$$\Delta(i\Omega) = \frac{1}{|\Omega|^{\alpha}}\,. \tag{45}$$

We assume $0 < \text{Re}\,[\alpha] < 1/3$ to ensure a convergent integral in (43), and then we have

$$E(\alpha) = \mathcal{K}\frac{\pi^2\left(3\cot\left(\frac{\pi\alpha}{2}\right)+\sqrt{3}\right)\sec\left(\pi\left(\alpha+\frac{1}{6}\right)\right)}{9\Gamma\left(\frac{1}{3}\right)\Gamma(1-\alpha)\Gamma\left(\alpha+\frac{2}{3}\right)}\,, \tag{46}$$

a result analogous to (**??**). The solution of $E(\alpha) = 1$ is shown in Fig. 5. For $\mathcal{K} = 1$, setting $E(\alpha) = 1$ indicates a complex scaling dimension $\alpha = 1/6 \pm i \times 0.53734\ \ldots$, which implies that a pairing instability exists and the ground state is superconducting. As the value of $\mathcal{K}$ is reduced, the magnitude of the imaginary part of α also reduces, going to zero at $\mathcal{K} = \mathcal{K}^* = 0.12038\ \ldots$, at which point $\alpha = 1/6$ exactly. For $0 < \mathcal{K} < \mathcal{K}^*$, $E = 1$ has two solutions with purely real α: α_1, with $0 < \alpha_1 < 1/6$ and $\alpha_2 = 1/3 - \alpha_1$, indicating the absence of a superconducting instability arising purely out of the relevant operators in the low energy critical theory, when the repulsive interaction is strong enough. Arguments have been made [8] that α_1 is the correct choice for the scaling dimension. For $\mathcal{K} < 0$, there is no solution for $E = 1$; therefore, there is no superconducting instability, and the scaling dimension of the pairing vertex equals its bare value.

To summarize, the above results imply a pairing instability for the Ising ferromagnet with purely attractive interactions ($\mathcal{K} = 1$), but no pairing instability for the gauge field case with purely repulsive interactions ($\mathcal{K} = -1$). If we have a combination of repulsive and attractive interactions, then $\mathcal{K}$ interpolates between 1 and -1, and there is no pairing instability for $\mathcal{K} < \mathcal{K}^* = 0.12038$. The critical Fermi surface state is stable for all $\mathcal{K} < \mathcal{K}^*$, and has a non-trivial dimension for pairing fluctuations in the regime $0 < \mathcal{K} < \mathcal{K}^*$ shown in Fig. 5.

We conclude by noting that it is possible to also consider the scaling of other composite operators from the product of two fermion fields, as in Section **??** for the SYK model. It turns out there is no non-trivial scaling of operators made by the product of $\psi_+^\dagger$ and ψ_+ because the analog of the k_x integral in (40) vanishes. However, there is interesting behavior in $\psi_+^\dagger \psi_-$, which is an operator with wavevector $2k_F$: this has been studied in Ref. [8].

V. TRANSPORT

One of the primary motivations for the intense study of critical Fermi surfaces has been the hope that it can lead to a theory of the iconic linear-T resistivity of strange metals (see Section **??**). However, the theory presented so far cannot describe such observations. The key point is that the important singular processes in such a theory can all be expressed in terms of a continuum field theory, such as that in (25), which conserves total momentum. In the absence of particle-hole symmetry, any state with a non-zero momentum has a non-zero current and vice-versa: consequently if we set up a state with a non-zero current, the non-zero total momentum of such a state will prevent the current from decaying to zero. In other words, the resistivity will vanish [22–26].

This effect can be viewed as one analogous to phonon drag [27, 28]. However, because of the weak electron-phonon coupling, phonon drag is significant only in the cleanest samples [29]. On the other hand, the coupling in the critical Fermi surface is so strong that the individual fermions and and bosons lose their identity and there are no quasiparticle excitations. Thus we cannot separately consider the momentum carried by the fermions and bosons.

A computation of the conductivity in the large N limit described above requires a summation of ladder diagrams which is described in Ref. [30]. Such an analysis leads only to a delta function in the conductivity at $T = 0$

$$\mathrm{Re}\,\sigma(\omega) = D_1 \delta(\omega)\,, \tag{47}$$

and the anomalous self energy of the electron in (21) does not show up. A subtle but important point is that this analysis of the conductivity cannot be carried out in the patch field theory of Section I C, and requires retaining additional terms in the fermion and boson dispersions [30]. To remove the delta function in (47), we need a mechanism to relax the momentum. Studies have examined the influence of umklapp scattering [31, 32], but here we focus on the promising results [30, 33] obtained by including spatial disorder.

The most important source of spatial disorder in the theory of disordered Fermi liquids is potential scattering, and so it is natural to include that here in the present theory. A form amenable to the large N limit being described here is the random potential action

$$\mathcal{S}_v = \frac{1}{\sqrt{N}} \sum_{\alpha,\beta=1}^{N} \int d^2r d\tau \, v_{\alpha\beta}(\boldsymbol{r}) \psi_\alpha^\dagger(\boldsymbol{r},\tau)\psi_\beta(\boldsymbol{r},\tau)$$
$$\overline{v_{\alpha\beta}(\boldsymbol{r})} = 0\,, \quad \overline{v_{\alpha\beta}^*(\boldsymbol{r}) v_{\gamma\delta}(\boldsymbol{r}')} = v^2 \, \delta(\boldsymbol{r}-\boldsymbol{r}')\delta_{\alpha\gamma}\delta_{\beta\delta} \tag{48}$$

The solution of the corresponding large N saddle point equations shows [33] that the boson polarizibility in (18) is replaced by

$$\Pi(\boldsymbol{q}, i\Omega_n) \sim -\frac{g^2}{v^2}|\Omega_n|, \tag{49}$$

which leads to $z = 2$ behavior in the boson propagator, with $[D(\boldsymbol{q}, i\Omega_n)]^{-1} \sim q^2 + \gamma|\Omega_n|$. The corresponding fermion self energy is modified from (21): it a familiar elastic impurity scattering contribution Σ_v also present in a disordered Fermi liquid, along with an inelastic term Σ_g [30] with the 'marginal Fermi liquid' form [34]

$$\Sigma_v(i\omega_n) \sim -iv^2 \mathrm{sgn}(\omega_n), \quad \Sigma_g(i\omega_n) \sim -\frac{g^2}{v^2}\omega_n \ln(1/|\omega_n|)\,. \tag{50}$$

Despite the promising singularity in Σ_g, (50) does not translate [30] into interesting behavior in the transport: the scattering is mostly forward, and the resistivity is Fermi liquid-like with $\rho(T) = \rho(0) + AT^2$.

Much more interesting and appealing behavior results when we add spatial randomness in the Yukawa coupling. Such randomness will be generated by the potential randomness $v_{\alpha\beta}(x)$ considered above, but it has to included at the outset in the large N limit. More explicitly, we recall that the Yukawa coupling invariably arises from a Hubbard-Stratonovich decoupling of a four-fermion interaction: we can decouple such an interaction via a ϕ^2 term which is spatially uniform, and then all the spatial disorder is transferred to the Yukawa term.

So we *add* to the spatially independent Yukawa couplings $g_{\alpha\beta\gamma}$ in (2) a second coupling $g'_{\alpha\beta\gamma}(\boldsymbol{r})$ which has both spatial and flavor randomness with action

$$\mathcal{S}_{g'} = \frac{1}{N} \int d^2r d\tau \, g'_{\alpha\beta\gamma}(\boldsymbol{r}) \psi_\alpha^\dagger(\boldsymbol{r},\tau)\psi_\beta(\boldsymbol{r},\tau)\phi_\gamma(\boldsymbol{r},\tau) \tag{51}$$
$$\overline{{g'}_{\alpha\beta\gamma}(\boldsymbol{r})} = 0\,, \quad \overline{{g'}_{\alpha\beta\gamma}^*(\boldsymbol{r}) g'_{\delta\rho\sigma}(\boldsymbol{r}')} = {g'}^2 \, \delta(\boldsymbol{r}-\boldsymbol{r}')\delta_{\alpha\delta}\delta_{\beta\rho}\delta_{\gamma\sigma}\,,$$

Then we obtain additional contributions to the boson and fermion self energies [33]

$$\Pi_{g'}(\boldsymbol{q}, i\Omega_n) \sim -g'^2|\Omega_n|\,, \quad \Sigma_{g'}(i\omega_n) \sim -ig'^2\omega_n \ln(1/|\omega_n|)\,. \tag{52}$$

Now the marginal Fermi liquid self energy does contribute significantly to transport [33], with a linear-T resistivity $\sim g'^2 T$, while the residual resistivity is determined primarily by v. It is notable that it is the disorder in the interactions, v, which determines the slope of the linear-T resistivity, while it is the potential scattering disorder which determines the residual resistivity. Other attractive features of this theory are that it has an anomalous optical conductivity $\sigma(\omega)$ with $\text{Re}[1/\sigma(\omega)] \sim \omega$ and a $T\ln(1/T)$ specific heat [33].

---

[1] N. F. Berk and J. R. Schrieffer, *Effect of ferromagnetic spin correlations on superconductivity*, Phys. Rev. Lett. **17**, 433 (1966).

[2] S. Doniach and S. Engelsberg, *Low-Temperature Properties of Nearly Ferromagnetic Fermi Liquids*, Phys. Rev. Lett. **17**, 750 (1966).

[3] X. Y. Xu, K. Sun, Y. Schattner, E. Berg, and Z. Y. Meng, *Non-Fermi Liquid at (2+1)D Ferromagnetic Quantum Critical Point*, Physical Review X **7**, 031058 (2017), arXiv:1612.06075 [cond-mat.str-el].

[4] X. Y. Xu, A. Klein, K. Sun, A. V. Chubukov, and Z. Y. Meng, *Identification of non-Fermi liquid fermionic self-energy from quantum Monte Carlo data*, npj Quantum Materials **5**, 65 (2020), arXiv:2003.11573 [cond-mat.str-el].

[5] S.-S. Lee, *Recent Developments in Non-Fermi Liquid Theory*, Annual Review of Condensed Matter Physics **9**, 227 (2018), arXiv:1703.08172 [cond-mat.str-el].

[6] I. Esterlis and J. Schmalian, *Cooper pairing of incoherent electrons: an electron-phonon version of the Sachdev-Ye-Kitaev model*, Phys. Rev. B **100**, 115132 (2019), arXiv:1906.04747 [cond-mat.str-el].

[7] E. E. Aldape, T. Cookmeyer, A. A. Patel, and E. Altman, *Solvable theory of a strange metal at the breakdown of a heavy Fermi liquid*, Phys. Rev. B **105**, 235111 (2022), arXiv:2012.00763 [cond-mat.str-el].

[8] I. Esterlis, H. Guo, A. A. Patel, and S. Sachdev, *Large N theory of critical Fermi surfaces*, Phys. Rev. B **103**, 235129 (2021), arXiv:2103.08615 [cond-mat.str-el].

[9] J. A. Damia, M. Solís, and G. Torroba, *How non-Fermi liquids cure their infrared divergences*, Phys. Rev. B **102**, 045147 (2020), arXiv:2004.05181 [cond-mat.str-el].

[10] Y. Wang, A. Abanov, B. L. Altshuler, E. A. Yuzbashyan, and A. V. Chubukov, *Superconductivity near a Quantum-Critical Point: The Special Role of the First Matsubara Frequency*, Phys. Rev. Lett. **117**, 157001 (2016), arXiv:1606.01252 [cond-mat.supr-con].

[11] S.-S. Lee, *Low-energy effective theory of Fermi surface coupled with U(1) gauge field in 2+1 dimensions*, Phys. Rev. B **80**, 165102 (2009), arXiv:0905.4532 [cond-mat.str-el].

[12] M. A. Metlitski and S. Sachdev, *Quantum phase transitions of metals in two spatial dimensions. I. Ising-nematic order*, Phys. Rev. B **82**, 075127 (2010), arXiv:1001.1153 [cond-mat.str-el].

[13] S. Powell, S. Sachdev, and H. P. Büchler, *Depletion of the Bose-Einstein condensate in Bose-Fermi mixtures*, Phys. Rev. B **72**, 024534 (2005), cond-mat/0502299.

[14] P. Coleman, I. Paul, and J. Rech, *Sum rules and Ward identities in the Kondo lattice*, Phys. Rev. B **72**, 094430 (2005), cond-mat/0503001.

[15] J. Kim, I. R. Klebanov, G. Tarnopolsky, and W. Zhao, *Symmetry Breaking in Coupled SYK or Tensor Models*, Phys. Rev. X **9**, 021043 (2019), arXiv:1902.02287 [hep-th].

[16] I. R. Klebanov, A. Milekhin, G. Tarnopolsky, and W. Zhao, *Spontaneous Breaking of $U(1)$ Symmetry in Coupled Complex SYK Models*, JHEP **11**, 162, arXiv:2006.07317 [hep-th].

[17] Y.-H. Zhang and S. Sachdev, *Deconfined criticality and ghost Fermi surfaces at the onset of antiferromagnetism in a metal*, Phys. Rev. B **102**, 155124 (2020), arXiv:2006.01140 [cond-mat.str-el].

[18] E.-G. Moon and A. Chubukov, *Quantum-critical Pairing with Varying Exponents*, Journal of Low Temperature Physics **161**, 263 (2010), arXiv:1005.0356 [cond-mat.supr-con].

[19] A. Abanov and A. V. Chubukov, *Interplay between superconductivity and non-Fermi liquid at a quantum critical point in a metal. I. The γ model and its phase diagram at T =0 : The case* $0 < \gamma < 1$, Phys. Rev. B **102**, 024524 (2020), arXiv:2004.13220 [cond-mat.str-el].

[20] Y.-M. Wu, A. Abanov, Y. Wang, and A. V. Chubukov, *Interplay between superconductivity and non-Fermi liquid at a quantum critical point in a metal. II. The γ model at a finite T for* $0 < \gamma < 1$, Phys. Rev. B **102**, 024525 (2020), arXiv:2006.02968 [cond-mat.supr-con].

[21] A. V. Chubukov and A. Abanov, *Pairing by a Dynamical Interaction in a Metal*, Soviet Journal of Experimental and Theoretical Physics **132**, 606 (2021), arXiv:2012.11777 [cond-mat.supr-con].

[22] S. A. Hartnoll, P. K. Kovtun, M. Muller, and S. Sachdev, *Theory of the Nernst effect near quantum phase transitions in condensed matter, and in dyonic black holes*, Phys. Rev. B **76**, 144502 (2007), arXiv:0706.3215 [cond-mat.str-el].

[23] D. L. Maslov, V. I. Yudson, and A. V. Chubukov, *Resistivity of a Non-Galilean-Invariant Fermi Liquid near Pomeranchuk Quantum Criticality*, Phys. Rev. Lett. **106**, 106403 (2011), arXiv:1012.0069 [cond-mat.str-el].

[24] S. A. Hartnoll, R. Mahajan, M. Punk, and S. Sachdev, *Transport near the Ising-nematic quantum critical point of metals in two dimensions*, Phys. Rev. **B89**, 155130 (2014), arXiv:1401.7012 [cond-mat.str-el].

[25] A. Eberlein, I. Mandal, and S. Sachdev, *Hyperscaling violation at the Ising-nematic quantum critical point in two dimensional metals*, Phys. Rev. B **94**, 045133 (2016), arXiv:1605.00657 [cond-mat.str-el].

[26] S. A. Hartnoll, A. Lucas, and S. Sachdev, *Holographic quantum matter*, MIT Press, Cambridge MA (2016), arXiv:1612.07324 [hep-th].

[27] R. Peierls, *Zur Theorie der elektrischen und thermischen Leitfähigkeit von Metallen*, Annalen der Physik **396**, 121 (1930).

[28] R. Peierls, *Zur Frage des elektrischen Widerstandsgesetzes für tiefe Temperaturen*, Annalen der Physik **404**, 154 (1932).

[29] C. W. Hicks, A. S. Gibbs, A. P. Mackenzie, H. Takatsu, Y. Maeno, and E. A. Yelland, *Quantum Oscillations and High Carrier Mobility in the Delafossite* $PdCoO_2$, Phys. Rev. Lett. **109**, 116401 (2012), arXiv:1207.5402 [cond-mat.str-el].

[30] H. Guo, A. A. Patel, I. Esterlis, and S. Sachdev, *Large-N theory of critical Fermi surfaces. II. Conductivity*, Phys. Rev. B **106**, 115151 (2022), arXiv:2207.08841 [cond-mat.str-el].

[31] X. Wang and E. Berg, *Scattering mechanisms and electrical transport near an Ising nematic quantum critical point*, Phys. Rev. B **99**, 235136 (2019), arXiv:1902.04590 [cond-mat.str-el].

[32] P. A. Lee, *Low-temperature T-linear resistivity due to umklapp scattering from a critical mode*, Phys. Rev. B **104**, 035140 (2021), arXiv:2012.09339 [cond-mat.str-el].

[33] A. A. Patel, H. Guo, I. Esterlis, and S. Sachdev, *Universal theory of strange metals from spatially random interactions*, Science **381**, 6659 (2023), arXiv:2203.04990 [cond-mat.str-el].

[34] C. M. Varma, P. B. Littlewood, S. Schmitt-Rink, E. Abrahams, and A. E. Ruckenstein, *Phenomenology of the normal state of Cu-O high-temperature superconductors*, Phys. Rev. Lett. **63**, 1996 (1989).